

# The STING ligand cGAMP potentiates the efficacy of vaccine-induced CD8<sup>+</sup> T cells

Alice Gutjahr,<sup>1,2,3</sup> Laura Papagno,<sup>4</sup> Francesco Nicoli,<sup>4</sup> Tomohiro Kanuma,<sup>5</sup> Nozomi Kuse,<sup>6</sup> Mariela Pires Cabral-Piccin,<sup>4</sup> Nicolas Rochereau,<sup>3</sup> Emma Gostick,<sup>7</sup> Thierry Lioux,<sup>3</sup> Eric Perouzel,<sup>3</sup> David A. Price,<sup>7</sup> Masafumi Takiguchi,<sup>6</sup> Bernard Verrier,<sup>2</sup> Takuya Yamamoto,<sup>5,6</sup> Stéphane Paul,<sup>1</sup> and Victor Appay<sup>4,8</sup>

<sup>1</sup>Groupe Immunité des Muqueuses et Agents Pathogènes, INSERM, Centre d'Investigation Clinique en Vaccinologie 1408, Faculté de Médecine de Saint-Etienne, Saint-Etienne, France. <sup>2</sup>Laboratoire de Biologie Tissulaire et d'Ingénierie Thérapeutique, Unité Mixte de Recherche 5305, Université Lyon 1, CNRS, Lyon, France. <sup>3</sup>InvivoGen, Toulouse, France. <sup>4</sup>Sorbonne Université, INSERM, Centre d'Immunologie et des Maladies Infectieuses (CIMI-Paris), Paris, France. <sup>5</sup>Laboratory of Immunosenescence, National Institutes of Biomedical Innovation, Health and Nutrition, Osaka, Japan. <sup>6</sup>Center for AIDS Research, Kumamoto University, Kumamoto, Japan. <sup>7</sup>Division of Infection and Immunity, Cardiff University School of Medicine, Cardiff, United Kingdom. <sup>8</sup>International Research Center of Medical Sciences (IRCMS), Kumamoto University, Kumamoto, Japan.

**Pathogen recognition receptor (PRR) agonists are currently being developed and tested as adjuvants in various formulations to optimize the immunogenicity and efficacy of vaccines. Using an original in vitro approach to prime naive precursors from unfractionated human peripheral blood mononuclear cells, we assessed the influence of cyclic guanosine monophosphate-adenosine monophosphate (cGAMP), a ligand for the stimulator of interferon genes (STING), on the induction of antigen-specific CD8<sup>+</sup> T cells. We found that 2'3'-cGAMP and 3'3'-cGAMP were especially potent adjuvants in this system, driving the expansion and maturation of functionally replete antigen-specific CD8<sup>+</sup> T cells via the induction of type I IFNs. The biological relevance of these findings was confirmed in vivo using two mouse models, in which 2'3'-cGAMP-adjuvanted vaccination elicited protective antitumor or antiviral CD8<sup>+</sup> T cell responses. These results identify particular isoforms of cGAMP as effective adjuvants that may find utility in the development of novel immunotherapies and vaccines.**

## Introduction

CD8<sup>+</sup> T cells are required for protective immunity against cancer and intracellular pathogens, but it remains unclear how best to induce functionally adept effector and memory responses, which have been shown to correlate with favorable disease outcomes (1). The functional attributes of de novo CD8<sup>+</sup> T cell populations are determined by early signaling events that drive the activation and expansion of naive precursors in response to TCR-mediated recognition of cognate antigen in the presence of costimulatory signals, typically provided in a conducive spatiotemporal format by DCs. Pathogen recognition receptor (PRR) ligands can further modulate these signals and thereby enhance the priming process to elicit more robust adaptive immune responses (2, 3). Agonist ligands for the stimulator of interferon genes (STING) have shown promise in this context (4), especially as vaccine adjuvants in preclinical models of cancer immunotherapy (5–8). However, the potential utility of these novel immunomodulators remains in doubt, because lymphocyte proliferation can be inhibited via the STING pathway (9). Common STING ligands include cyclic dinucleotides, such as 2'3'-cyclic guanosine monophosphate-adenosine monophosphate (2'3'-cGAMP), which is synthesized by cGAMP synthase (cGAS) upon detection of cytosolic double-stranded DNA; and 3'3'-cGAMP, which is secreted by intracellular pathogenic bacteria (10). In this study, we show that these isoforms of cGAMP act as potent adjuvants in vitro and in vivo, enhancing the induction of functional antigen-specific CD8<sup>+</sup> T cell responses in humans and the induction of protective antigen-specific CD8<sup>+</sup> T cell responses in mice.

**Conflict of interest:** TL and EP are employees of InvivoGen.

**Authorship note:** AG and LP; FN and TK; and TY, SP, and VA contributed equally to this work.

**Copyright:** © 2019 American Society for Clinical Investigation

**Submitted:** September 25, 2018

**Accepted:** February 14, 2019

**Published:** April 4, 2019.

**Reference information:** *JCI Insight*. 2019;4(7):e125107. <https://doi.org/10.1172/jci.insight.125107>.

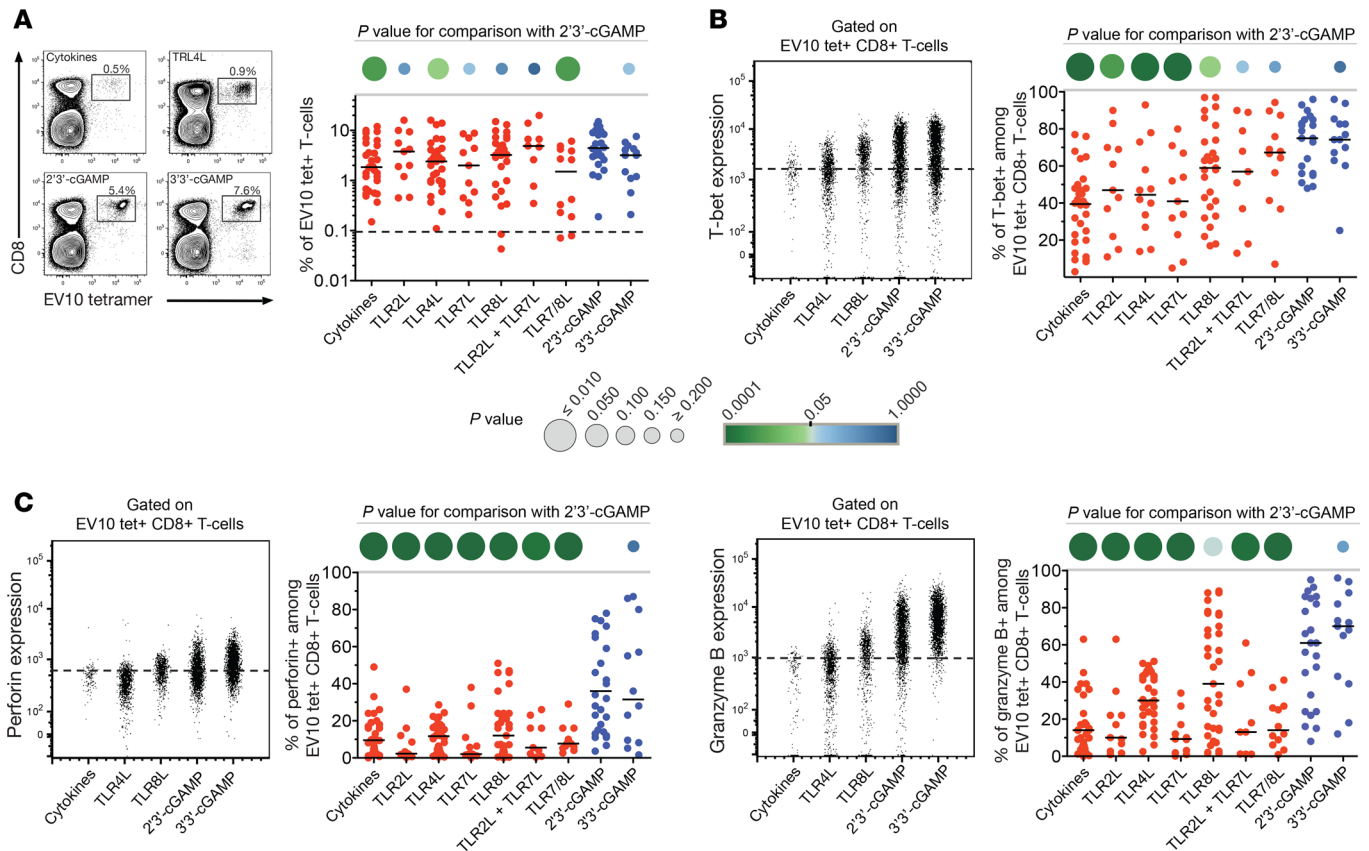


**Figure 1. STING ligands enhance the induction of effector CD8<sup>+</sup> T cells.** (A) Left: Representative flow cytometry data showing EV10-specific CD8<sup>+</sup> T cells expanded in the presence of Flt3 ligand and various adjuvants. Cytokines: TNF, IL-1 $\beta$ , IL-7, and PGE2. Plots are gated on viable CD3<sup>+</sup> events. Percentage values represent HLA-A2-EV10 tetramer<sup>+</sup> cells among total CD8<sup>+</sup> T cells. Right: Data summary. Each dot represents 1 HLA-A2<sup>+</sup> donor per condition. The dotted line shows the mean percentage of HLA-A2-EV10 tetramer<sup>+</sup> cells among total CD8<sup>+</sup> T cells incubated with cytokines in the absence of peptide ( $n = 20$ ). (B) Intracellular expression of T-bet among EV10-specific CD8<sup>+</sup> T cells primed as in A. Left: Representative flow cytometry plots gated on viable HLA-A2-EV10 tetramer<sup>+</sup> CD8<sup>+</sup> T cells. The dotted line shows the limit for positive expression. Right: data summary. Each dot represents 1 HLA-A2<sup>+</sup> donor per condition. (C) Intracellular expression of perforin and granzyme B among EV10-specific CD8<sup>+</sup> T cells primed as in A. Details as in B. Horizontal bars indicate median values. *P* values are represented as circles with variable size and color intensity (Mann-Whitney *U* test).

## Results

*cGAMP* enhances the induction of effector CD8<sup>+</sup> T cells *in vitro*. Using an *in vitro* approach to prime naive precursors from human PBMCs (11), we tested the effects of STING and TLR ligands on the induction of antigen-specific CD8<sup>+</sup> T cells. To minimize stochastic effects attributable to low precursor frequencies, we confined our investigation to the heteroclitic Melan-A epitope ELAGIGILTV<sub>26-35</sub> (EV10), which is recognized by very high frequencies of naive CD8<sup>+</sup> T cells in individuals expressing HLA-A\*0201 (abbreviated hereafter as HLA-A2) (12). Priming experiments were conducted with a longer peptide (EV20) incorporating the EV10 sequence to limit epitope display to DCs capable of antigen cross-presentation (13). Frequencies of EV10-specific CD8<sup>+</sup> T cells were quantified by tetramer staining on day 11. Modest quantitative differences were observed across the various priming conditions, but STING ligands, and in particular 2'3'-cGAMP, were among the most potent inducers of antigen-specific CD8<sup>+</sup> T cells (Figure 1A).

In parallel, we assessed intracellular expression of T-bet, which acts as a key transcriptional regulator of various effector functions, including the production of cytokines (e.g., IFN- $\gamma$ ) and cytotoxins (e.g., perforin and granzyme B) (14). The highest levels of T-bet were detected in EV10-specific CD8<sup>+</sup> T cells primed in the presence of 2'3'-cGAMP or 3'3'-cGAMP (Figure 1B). These cells also expressed very high levels of perforin and granzyme B, consistent with a potent effector profile (Figure 1C). No such effects were observed among tetramer<sup>-</sup> CD8<sup>+</sup> T cells (Supplemental Figure 1; supplemental material available online with this article; <https://doi.org/10.1172/jci.insight.125107DS1>). Moreover, 2'3'-cGAMP did not enhance the proliferation of purified or unpurified CD8<sup>+</sup> T cells in a nonspecific

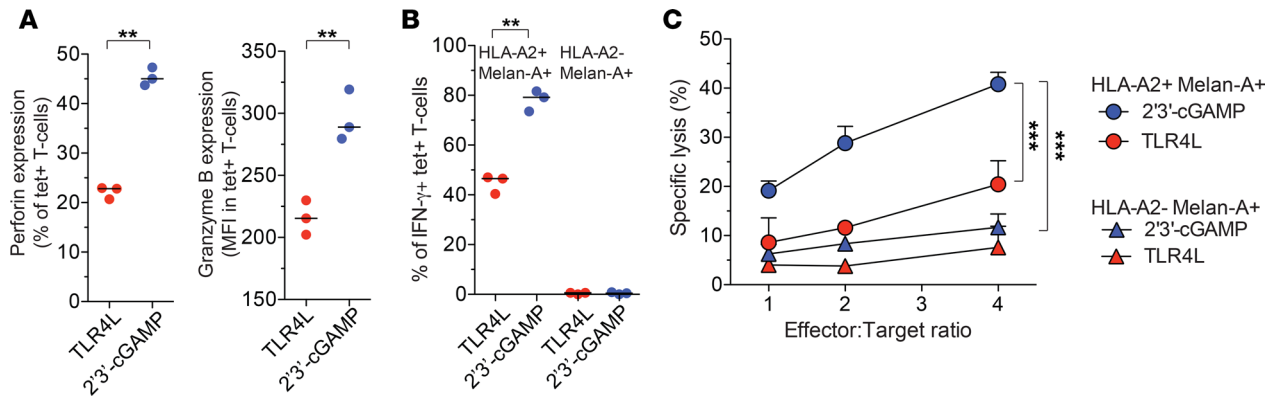


**Figure 2. STING ligands enhance the functionality of effector CD8<sup>+</sup> T cells.** (A) Intracellular expression of perforin and granzyme B among EV10-specific CD8<sup>+</sup> T cells primed in the presence of 2'3'-cGAMP or TLR4 and expanded for a further 2 weeks in culture after restimulation with EV10. (B) Intracellular expression of IFN-γ among EV10-specific CD8<sup>+</sup> T cells generated as in A after exposure to HLA-A2<sup>+</sup> or HLA-A2<sup>-</sup> melanoma cells (effector/target ratio 1:10). (C) Lysis of HLA-A2<sup>+</sup> or HLA-A2<sup>-</sup> melanoma cells by EV10-specific CD8<sup>+</sup> T cells generated as in A. Error bars indicate mean ± SEM (n = 3 replicates). \*\*P < 0.01, \*\*\*P < 0.001 (unpaired t test).

manner and actually inhibited the proliferation of purified CD8<sup>+</sup> T cells stimulated via cross-ligation of CD3, which mimics the productive engagement of TCRs (Supplemental Figure 2).

To confirm these findings, we tested the ability of EV10-specific CD8<sup>+</sup> T cells to kill melanoma cell lines, which naturally express the cognate epitope derived from Melan-A. For this purpose, CD8<sup>+</sup> T cells primed in the presence of 2'3'-cGAMP or TLR4L were expanded for a further 2 weeks in culture after restimulation with EV10. Perforin and granzyme B expression levels remained higher among 2'3'-cGAMP-primed EV10-specific CD8<sup>+</sup> T cells relative to TLR4L-primed EV10-specific CD8<sup>+</sup> T cells (Figure 2A). After exposure to HLA-A2<sup>+</sup> Melan-A<sup>+</sup> cells, higher frequencies of 2'3'-cGAMP-primed EV10-specific CD8<sup>+</sup> T cells produced IFN-γ relative to TLR4L-primed EV10-specific CD8<sup>+</sup> T cells, consistent with a durable and robust effector profile (Figure 2B). In line with these observations, 2'3'-cGAMP-primed EV10-specific CD8<sup>+</sup> T cells also killed HLA-A2<sup>+</sup> Melan-A<sup>+</sup> cells, but not HLA-A2<sup>-</sup> Melan-A<sup>+</sup> cells, more efficiently than TLR4L-primed EV10-specific CD8<sup>+</sup> T cells (Figure 2C).

Collectively, these data indicate that cGAMP enhances the induction of effector CD8<sup>+</sup> T cells in an antigen-dependent manner, and that this adjuvant-like activity overrides any direct inhibitory effects of cGAMP on the proliferation of CD8<sup>+</sup> T cells.

*cGAMP triggers strong type I IFN responses to prime effector CD8<sup>+</sup> T cells in vitro.* To gain mechanistic insights into the priming activity of cGAMP, we stimulated human monocyte-derived DCs (moDCs) with 2'3'-cGAMP or 3'3'-cGAMP. Gene expression analysis revealed that these ligands induced similar transcriptional profiles (Supplemental Figure 3). Of particular note, transcripts encoding type I and type II IFNs, as well as the proinflammatory cytokines IL-1, IL-6, IL-12, and IP-10, were overexpressed in cGAMP-stimulated moDCs relative to unstimulated moDCs, whereas transcripts encoding various MAPKs and TLRs were underexpressed in cGAMP-stimulated moDCs relative to unstimulated moDCs (Figure 3A). In line with the mRNA expression data, 2'3'-cGAMP and 3'3'-cGAMP also induced equivalent levels of maturation among moDCs, characterized by surface upregulation of CD40, CD80, CD86, and HLA-DR (Figure 3B).

Stimulation of PBMCs with 2'3'-cGAMP or 3'3'-cGAMP induced a distinct cytokine secretion profile, characterized by high levels of IFN-α and IFN-γ, intermediate levels of IL-6 and TNF, and low levels of IL-10 and IL-12 (Figure 4A and Supplemental Figure 4). Adjuvants that elicit such type I IFN responses have been linked with effector polarization among CD8<sup>+</sup> T cells (15). In our in vitro system, IFN-α enhanced the induction of effector CD8<sup>+</sup> T cells specific for EV10, consistent with the ability of this cytokine to upregulate T-bet (14, 16), whereas minimal effects were observed with IFN-γ and IL-12 (Figure 4B). Moreover, type I IFN-blocking antibodies inhibited the expansion and functional maturation of EV10-specific CD8<sup>+</sup> T cells primed in the presence of 2'3'-cGAMP (Figure 4C). The expansion of EV10-specific CD8<sup>+</sup> T cells driven by 2'3'-cGAMP was also inhibited in the presence of IL-10, which to a lesser extent impaired the upregulation of T-bet and the acquisition of granzyme B (Figure 4D).

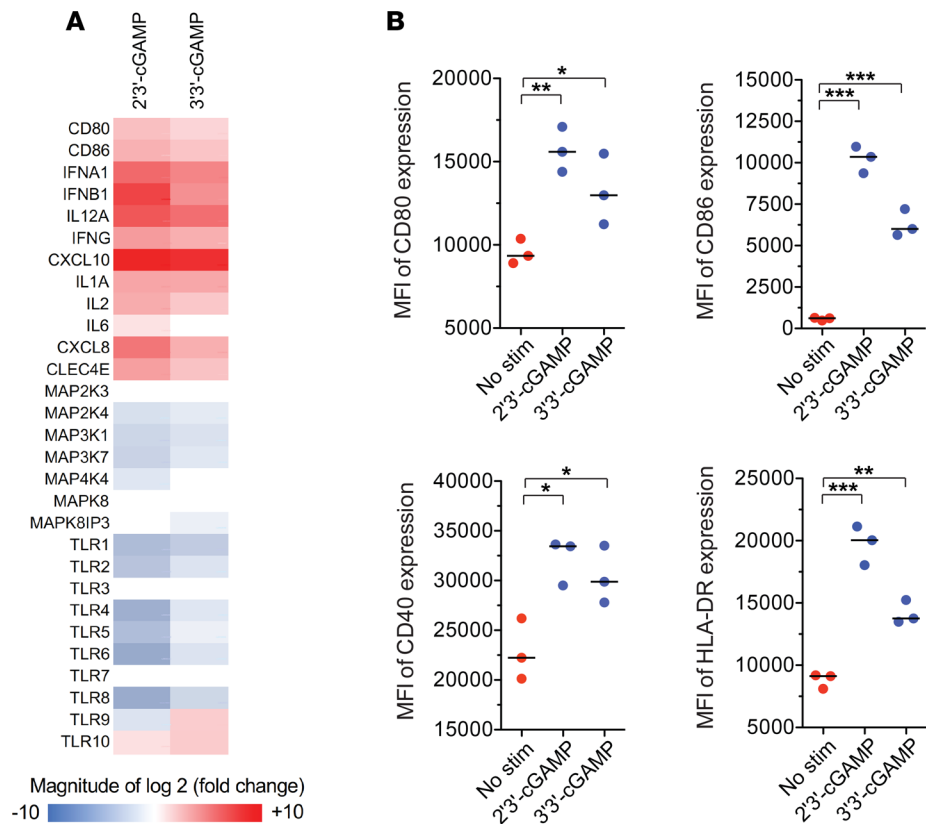


**Figure 3. STING ligands drive the maturation of DCs.** (A) Expression profile of PRR pathway genes in CD1a<sup>+</sup>CD14<sup>-</sup> moDCs 24 hours after stimulation with 2'3'-cGAMP or 3'3'-cGAMP at concentrations of 10  $\mu$ g/ml. Data are shown relative to unstimulated moDCs from the same donor. stim, stimulation. (B) Expression of maturation markers on CD1a<sup>+</sup>CD14<sup>-</sup> moDCs stimulated with 2'3'-cGAMP or 3'3'-cGAMP at concentrations of 10  $\mu$ g/ml. Error bars indicate mean  $\pm$  SEM ( $n = 3$  replicates). \* $P < 0.05$ , \*\* $P < 0.01$ , \*\*\* $P < 0.001$  (unpaired  $t$  test).

Collectively, these findings indicate that cGAMP enhances the induction and functional maturation of antigen-specific CD8<sup>+</sup> T cells via an indirect mechanism that involves type I IFNs.

*Intramuscular vaccination with 2'3'-cGAMP induces potent antitumor CD8<sup>+</sup> T cells in vivo.* To probe the biological relevance of 2'3'-cGAMP-enhanced CD8<sup>+</sup> T cell immunity in vivo, we vaccinated C57BL/6J mice intramuscularly with OVA, either alone or together with various adjuvants, and characterized the expansion and functional properties of CD8<sup>+</sup> T cells specific for the H-2K<sup>b</sup>-restricted OVA epitope SIINFEKL (SL8). The highest frequencies of SL8-specific CD8<sup>+</sup> T cells were observed after vaccination with OVA plus 2'3'-cGAMP or OVA plus AddaVax, an MF59-like squalene adjuvant (Figure 5A). However, SL8-specific CD8<sup>+</sup> T cells generated in the presence of 2'3'-cGAMP exhibited greater functionality than SL8-specific CD8<sup>+</sup> T cells generated in the presence of AddaVax, measured in terms of IFN- $\gamma$  production after restimulation with SL8 (Figure 5B).

Mice vaccinated with OVA alone, OVA plus 2'3'-cGAMP, or OVA plus AddaVax were then injected subcutaneously with the OVA<sup>+</sup> tumor cell line EG7, which can be controlled by SL8-specific CD8<sup>+</sup> T cells. Tumor growth was inhibited more effectively in mice vaccinated with OVA plus 2'3'-cGAMP relative to mice vaccinated with OVA plus AddaVax, despite equivalent frequencies of SL8-specific CD8<sup>+</sup> T cells, and vaccination with OVA plus AddaVax conferred no significant advantages over vaccination with OVA alone (Figure 5C).

Collectively, these data indicate that cGAMP enhances the induction and functional maturation of antigen-specific CD8<sup>+</sup> T cells in vivo, leading to greater immune protection in a tumor model.

*Intranasal vaccination with 2'3'-cGAMP induces potent antiviral CD8<sup>+</sup> T cells in vivo.* To confirm the utility of 2'3'-cGAMP as a superior adjuvant, we vaccinated CB6F1 mice intranasally with HIV-1 Gag p24 nanoparticles (NP-p24), either alone or together with 2'3'-cGAMP. The induction of CD8<sup>+</sup> T cells specific for the H-2K<sup>d</sup>-restricted HIV-1 Gag p24 epitope AMQMLKETI (AI9) was monitored using

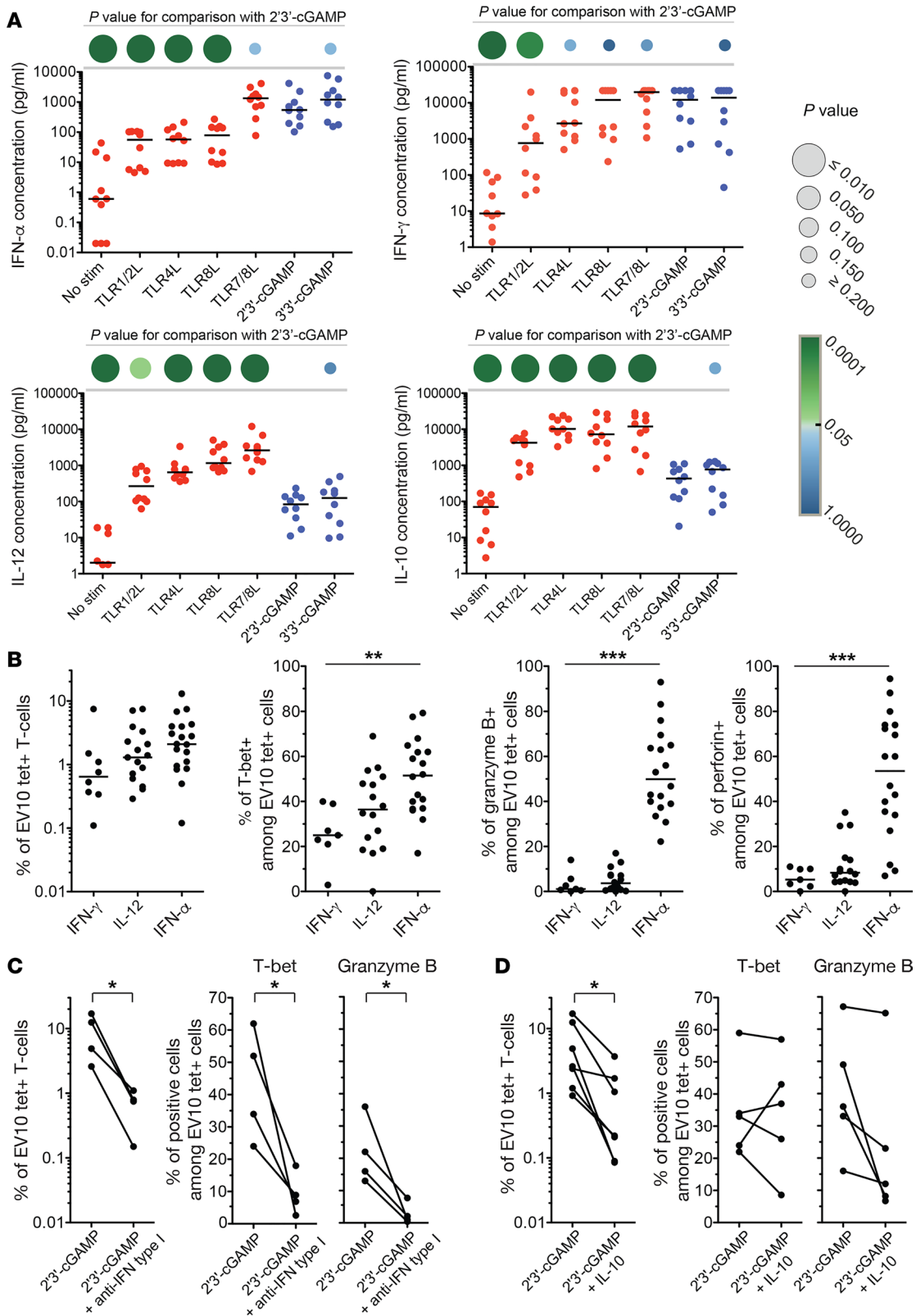


**Figure 4. STING ligands elicit a type I IFN response.** (A) Extracellular concentrations of various cytokines secreted by PBMCs in response to overnight stimulation with various PRR ligands. Each dot represents 1 donor per condition. Horizontal bars indicate median values. *P* values are represented as circles with variable size and color intensity (Mann-Whitney *U* test). (B) Frequency of EV10-specific CD8<sup>+</sup> T cells and intracellular expression of T-bet, perforin, and granzyme B among EV10-specific CD8<sup>+</sup> T cells primed in the presence of IFN- $\alpha$  (0.1  $\mu$ g/ml), IFN- $\gamma$  (0.1  $\mu$ g/ml), or IL-12 (0.1  $\mu$ g/ml). Each dot represents 1 HLA-A2<sup>+</sup> donor per condition. Horizontal bars indicate median values. \*\**P* < 0.01, \*\*\**P* < 0.001 (Kruskal-Wallis test). (C and D) Frequency of EV10-specific CD8<sup>+</sup> T cells and intracellular expression of T-bet and granzyme B among EV10-specific CD8<sup>+</sup> T cells primed in the presence of 2'3'-cGAMP, either alone or together with type I IFN blocking antibodies (C) or IL-10 (0.1  $\mu$ g/ml) (D). \**P* < 0.05 (paired *t* test).

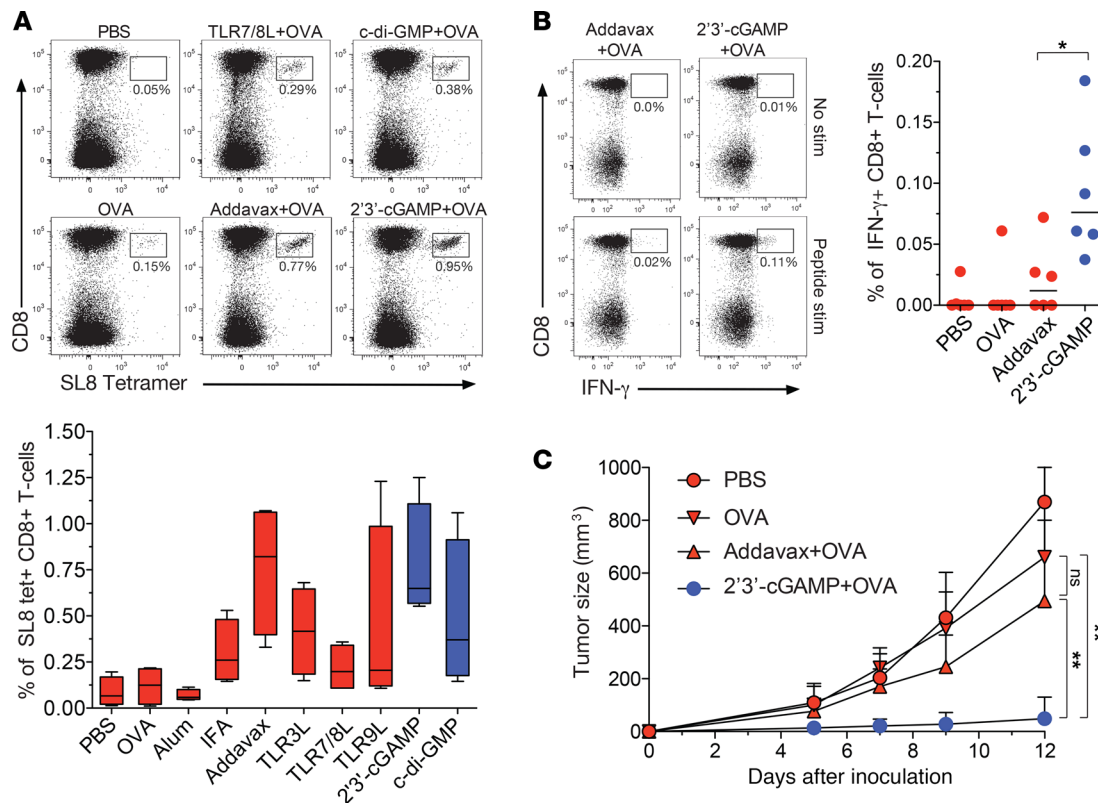


**Figure 5. cGAMP enhances the induction of protective antitumor CD8<sup>+</sup> T cells in vivo.** C57BL/6J mice were vaccinated intramuscularly with PBS (negative control) or OVA, either alone or together with various adjuvants, on days 0 and 14. **(A)** Top: Representative flow cytometry data showing SL8-specific CD8<sup>+</sup> T cells 1 week after the last vaccination. Plots are gated on viable CD3<sup>+</sup> events. Percentage values refer to H-2K<sup>b</sup>-SL8 tetramer<sup>+</sup> cells among total CD8<sup>+</sup> T cells. Bottom: Data summary ( $n = 4$  mice per group). **(B)** Left: Representative flow cytometry data showing IFN- $\gamma$  production among CD8<sup>+</sup> T cells restimulated with SL8 1 week after the last vaccination. Plots are gated on viable CD3<sup>+</sup> events. Percentage values refer to IFN- $\gamma$ <sup>+</sup> cells among total CD8<sup>+</sup> T cells. Right: Data summary. **(C)** Tumor size after subcutaneous injection of EG7 cells on day 21 ( $n = 10$  mice per group). Error bars indicate mean  $\pm$  SEM. \* $P < 0.05$ , \*\* $P < 0.01$  (unpaired  $t$  test).

the corresponding tetramer and IFN- $\gamma$  ELISpot assays. Higher frequencies of tetramer<sup>+</sup> CD8<sup>+</sup> T cells were observed after vaccination with NP-p24 plus 2'3'-cGAMP relative to vaccination with NP-p24 alone (Figure 6A), and these differences were even more pronounced in terms of IFN- $\gamma$  secretion after restimulation with AI9 (Figure 6B).

Mice were then challenged with a recombinant vaccinia virus expressing HIV-1 Gag (VV-Gag), which can be controlled by AI9-specific CD8<sup>+</sup> T cells. Significant weight loss was observed in mice vaccinated with PBS or NP-p24 alone, but not in mice vaccinated with NP-p24 plus 2'3'-cGAMP (Figure 6C). Viral replication was also controlled more effectively in mice vaccinated with NP-p24 plus 2'3'-cGAMP relative to mice vaccinated with NP-p24 alone (Figure 6D). Of note, mucosal and systemic HIV-1 Gag p24-specific IgA and IgG titers were very high in mice vaccinated with NP-p24 plus 2'3'-cGAMP, consistent with recent studies (17, 18), but remained undetectable in mice vaccinated with NP-p24 alone (Supplemental Figure 5).

Collectively, these findings indicate that cGAMP enhances the induction of holistic immune responses in vivo, leading to greater protection against subsequent viral challenge.

## Discussion

The recent discovery of the cGAS/STING pathway has unveiled new opportunities for immune modulation (4), with the potential to revolutionize vaccine delivery (19). In this study, we demonstrate that the STING ligands 2'3'-cGAMP and 3'3'-cGAMP act as potent adjuvants, enhancing the antigen-driven expansion and functional maturation of effector CD8<sup>+</sup> T cells in humans and mice. A mechanistic dissection of these effects in humans revealed that cGAMP elicits a type I IFN response and promotes the maturation of DCs, which have been shown previously to facilitate the cross-priming of antigen-specific

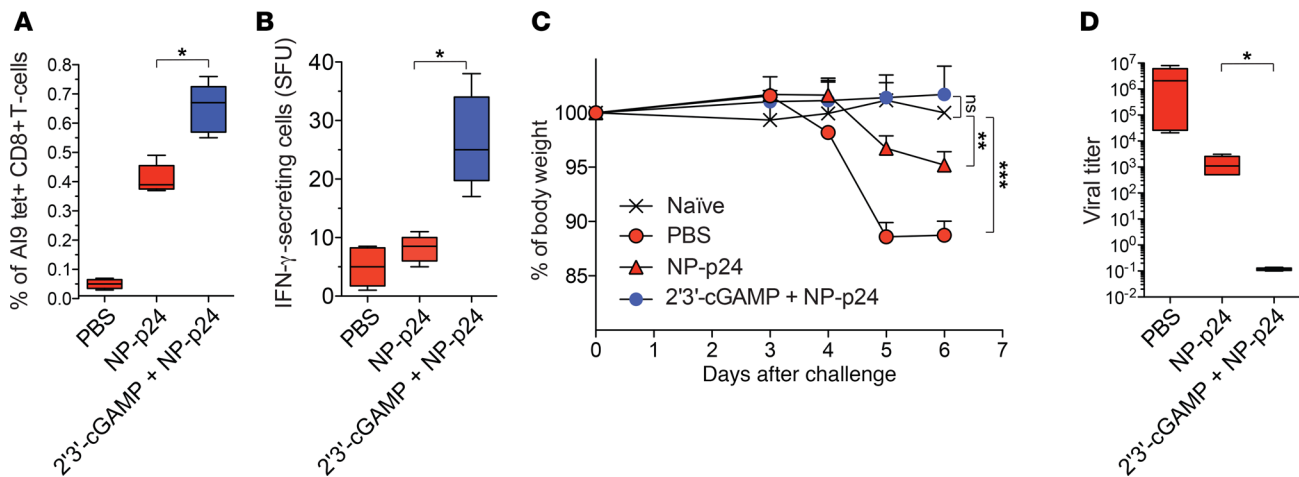


**Figure 6. cGAMP enhances the induction of protective antiviral CD8<sup>+</sup> T cells in vivo.** CB6F1 mice were vaccinated intranasally with PBS (negative control) or NP-p24, either alone or together with 2'3'-cGAMP, on days 0, 7, 14, and 21. **(A)** Frequency of H-2K<sup>d</sup>-A19 tetramer<sup>+</sup> CD8<sup>+</sup> T cells 1 week after the last vaccination. **(B)** Frequency of IFN- $\gamma$ -producing cells among splenocytes restimulated with A19 1 week after the last vaccination. Results are expressed as the number of spot-forming units (SFU) per  $3 \times 10^5$  splenocytes. **(C)** Weight loss after challenge with VV-Gag. Unchallenged naive mice were included as a negative control. **(D)** Viral titers 1 week after challenge with VV-Gag. Error bars indicate mean  $\pm$  SEM ( $n = 5$  mice per group). \* $P < 0.05$ , \*\* $P < 0.01$ , \*\*\* $P < 0.001$  (unpaired  $t$  test or Mann-Whitney  $U$  test).

CD8<sup>+</sup> T cells (20). Moreover, type I IFNs are known to induce the transcription factor T-bet, which is necessary for the development of effector CD8<sup>+</sup> T cells (14, 16).

The biological relevance of these findings was confirmed in vivo using two distinct experimental models, in which vaccinated mice were challenged with either a tumor cell line (EG7) or a replicating virus (VV-Gag). In both settings, 2'3'-cGAMP enhanced the induction of functionally superior CD8<sup>+</sup> T cells, leading to greater immune protection. Of note, these results also demonstrate the versatility of 2'3'-cGAMP as an adjuvant, given the different modes of delivery (solution versus solid phase) and the different routes of vaccination (intramuscular versus intranasal) in each model, as well as the coinduction of mucosal and systemic humoral immune responses. Moreover, toxicity may be limited in humans by the relative lack of a proinflammatory response, which contrasts with many other candidate vaccine adjuvants. Such risks may be further mitigated by incorporating 2'3'-cGAMP into nanoparticles with delivery agents such as amphiphiles or polymers that localize activity to secondary lymphoid organs (21, 22).

The results presented here identify cGAMP as a potent adjuvant for the induction of de novo CD8<sup>+</sup> T cell responses, potentially enabling novel immunotherapeutic and prophylactic approaches to the management of various cancers and infectious diseases. It could be especially fitted to prime effector CD8<sup>+</sup> T cells against tumor neoantigens identified in cancer patients. Moreover, the ability of cGAMP to elicit humoral immune responses in parallel, including the secretion of IgA at mucosal surfaces, may confer further advantages in the setting of certain viral infections, such as HIV-1 (23).

## Methods

**Peptides and tetramers.** All peptides were synthesized at >95% purity (Biosynthesis Inc.). The EV20 peptide (YTAAEELAGIGILTVILGVL, Melan-A<sub>21-40/A27L</sub>) was used for in vitro priming studies. Fluorochrome-labeled tetrameric complexes of HLA-A2-EV10 (ELAGIGILTV, Melan-A<sub>26-35/A27L</sub>), H-2K<sup>b</sup>-SL8 (SIINFEKL, OVA<sub>257-264</sub>), and H-2K<sup>d</sup>-A19 (AMQMLKETI, p24<sub>65-73</sub>) were purchased commercially (MBL International CliniSciences) or generated in-house as described previously (24, 25).

**In vitro priming of human antigen-specific CD8<sup>+</sup> T cells.** PBMCs were isolated and cryopreserved from venous blood samples donated by healthy HLA-A2<sup>+</sup> volunteers attending the Etablissement Français du Sang. Naive precursors specific for HLA-A2-EV10 were primed in vitro using an accelerated DC coculture protocol as described previously (11, 26). Briefly, thawed PBMCs were resuspended at  $5 \times 10^6$  cells/well in 24-well tissue culture plates containing AIM medium (Invitrogen) supplemented with Flt3L (50 ng/ml; R&D Systems) to mobilize resident DCs. After 24 hours (day 1), the Melan-A peptide EV20 (1  $\mu$ M) was added to the cultures, and DC maturation was induced

under different adjuvant conditions, including: (i) a standard cocktail of inflammatory cytokines comprising TNF (1000 U/ml), IL-1 $\beta$  (10 ng/ml), IL-7 (0.5 ng/ml), and prostaglandin E2 (PGE2; 1  $\mu$ M) (R&D Systems); (ii) various TLR ligands, namely TLR1/2 (1  $\mu$ g/ml), TLR2 (2.5  $\mu$ g/ml), TLR4 (0.1  $\mu$ g/ml), TLR7 (0.5  $\mu$ g/ml), TLR7/8 (5  $\mu$ g/ml), or TLR8 (0.5  $\mu$ g/ml) (InvivoGen); (iii) STING ligands 2'3'-cGAMP (10  $\mu$ g/ml) or 3'3'-cGAMP (10  $\mu$ g/ml) (InvivoGen); or (iv) various additional cytokines, namely IFN- $\alpha$  2a (0.1  $\mu$ g/ml; ImmunoTools), IFN- $\gamma$  (0.1  $\mu$ g/ml; R&D Systems), IL-10 (0.1  $\mu$ g/ml; BioLegend), or IL-12 (0.1  $\mu$ g/ml; R&D Systems). Optimal concentrations of PRR ligands were determined as sufficient to elicit a plateau effect in titration assays using reporter cell lines (HEK or RAW). The cultures were further supplemented on day 1 in some experiments with a combination of  $\alpha$ -IFN- $\alpha$  (20,000 NU/ml; Tebu-Bio) and  $\alpha$ -IFN- $\beta$  (5000 NU/ml; Tebu-Bio) to block the activity of type I IFNs. On day 2, FBS was added at a final v/v ratio of 10%. Medium was then replaced every 3 days with fresh RPMI 1640 enriched with 10% FBS (R10). Antigen-specific CD8<sup>+</sup> T cells were typically characterized on day 10 or day 11.

**Flow cytometry.** The following directly conjugated monoclonal antibodies were used to stain human CD8<sup>+</sup> T cells: (i)  $\alpha$ -CD3-ECD (clone UCHT1, Beckman Coulter); (ii)  $\alpha$ -CD8-APC-Cy7 (clone SK1) and  $\alpha$ -granzyme B-V450 (clone GB11) (BD Biosciences); (iii)  $\alpha$ -perforin-FITC (clone B-D48, BioLegend); and (iv)  $\alpha$ -T-bet-Alexa Fluor 647 (clone 4B10, eBioscience). Dead cells were identified using the amine-reactive viability dye Aqua (Life Technologies). Intracellular staining for T-bet was performed using a Transcription Factor Buffer Set (BD Pharmingen). Intracellular staining for perforin and granzyme B was compatible with this procedure. Staining with all other reagents was conducted according to standard protocols (27, 28). The following directly conjugated monoclonal antibodies were used to stain mouse CD8<sup>+</sup> T cells: (i)  $\alpha$ -CD3-APC-Fire750 (clone 17A2),  $\alpha$ -CD4-BV510 (clone GK1.5),  $\alpha$ -CD8a-BV570 (clone 53-6.7), and  $\alpha$ -IFN- $\gamma$ -Alexa Fluor 488 (clone XMG1.2) (BioLegend); and (ii)  $\alpha$ -CD44-PE-Cy5 (clone IM7, BD Biosciences). Proliferation was monitored using Cell Proliferation Dye eFluor 450 (CPD, eBioscience). Briefly, total PBMCs or magnetic bead-purified CD8<sup>+</sup> T cells were stained with CPD (20  $\mu$ M) for 10 minutes, then washed and stimulated with plate-bound  $\alpha$ -CD3. After 4 days, CPD dilution was evaluated in CD8<sup>+</sup> T cells. Data were acquired using LSR Fortessa or FACSCanto II flow cytometers (BD Biosciences) and analyzed with FlowJo software version 9.3.7 (Tree Star Inc.).

**Measurement of soluble factors.** Cytokines and chemokines were measured using a Luminex T200 instrument in combination with mouse or human Bio-Plex Immunoassay Kits (Bio-Rad). All concentrations were determined as the mean of 2 replicates. HIV-1 Gag p24-specific IgA and IgG titers were quantified by ELISA (29).

**In vitro killing assay.** The cytolytic activity of primed CD8<sup>+</sup> T cells was measured using an LDH Cytotoxicity Detection Kit (Clontech Takara). Effector cells were cocultured with target melanoma cell lines for 4 hours at 37°C. Spontaneous release of LDH was determined in supernatants from wells containing target cells only, and maximal release of LDH was determined in supernatants from wells containing 2.5% Triton X-100. Cytolytic activity (%) was calculated as (Experimental value – Spontaneous value) / (Maximal value – Spontaneous value)  $\times$  100.

**moDC stimulation and real-time PCR.** Monocytes were purified from human peripheral blood and differentiated into moDCs as described previously (30). After 6 days,  $1 \times 10^6$  moDCs per condition were incubated for 24 hours in the absence or presence of various ligands at individual concentrations of 10  $\mu$ g/ml. Cells were then stained with  $\alpha$ -CD1a-FITC (clone HI149) together with  $\alpha$ -CD40-PE (clone 5C3),  $\alpha$ -CD80-PE (clone L307),  $\alpha$ -CD86-PE (clone 2331), or  $\alpha$ -HLA-DR-PE (clone TU36) (BD Biosciences). Data were acquired using a FACSCanto I flow cytometer (BD Biosciences) and analyzed with FlowJo software version 9.3.7 (Tree Star Inc.). RNA was extracted from moDCs using an RNeasy Mini Kit (QIAGEN), and the expression of 84 genes was quantified using an RT<sup>2</sup> Profiler PCR Arrays Human Toll-Like Receptor Signaling Pathway Kit (QIAGEN).

**Mouse model 1: intramuscular vaccination and tumor challenge.** Six-week-old female C57BL/6J mice (CLEA Japan Inc.) were vaccinated intramuscularly on day 0 and day 14 with PBS or OVA (10  $\mu$ g; Seikagaku Kogyo), either alone or together with various TLR ligands, namely TLR3 (10  $\mu$ g/ml), TLR7/8 (10  $\mu$ g/ml), or TLR9 (10  $\mu$ g/ml), STING ligands 2'3'-cGAMP (10  $\mu$ g/ml) or c-di-GMP (10  $\mu$ g/ml), alum (final v/v ratio of 10%), IFA (final v/v ratio of 10%), or AddaVax (final v/v ratio of 10%) (all from InvivoGen). On day 21, mice were injected subcutaneously with  $1 \times 10^6$  EG7 cells in 100  $\mu$ l PBS. The OVA-expressing thymoma cell line EG7

(ATCC) was maintained at 37°C in RPMI 1640 supplemented with 10% FBS, 50 µg/ml penicillin/streptomycin, 0.05 mM 2-mercaptoethanol, 1 mM sodium pyruvate, 10 mM HEPES, and 1× nonessential amino acids (Life Technologies). Immunized mice were monitored prospectively for signs of toxicity, including weight loss and general deterioration. Tumor size was measured by length ( $L$ ), width ( $W$ ), and height ( $H$ ), and tumor volume ( $V$ ) was calculated as  $V = L \times W \times H$ .

*Mouse model 2: intranasal vaccination and viral challenge.* Seven-week-old female CB6F1 mice (Charles River) were anesthetized with isoflurane and vaccinated intranasally (31) with PBS (Gibco), HIV-1 Gag p24 (10 µg; PX Therapeutics) adsorbed onto PLA i-Particles (Adjuvatis) alone (NP-p24), or an identical dose of NP-p24 together with 2'3'-cGAMP (10 µg; InvivoGen). Three doses of each formulation were administered in a final volume of 20 µl at weekly intervals, followed by an equivalent booster dose after a further 3 weeks. Immunized mice were monitored prospectively for signs of toxicity, including weight loss and general deterioration. Biological fluids were recovered before and 1 week after each immunization to examine antibody production (29). Viral challenge was performed using a vDK1 recombinant vaccinia virus expressing HIV-1 Gag p24 (NIH AIDS Reagent Program) (32, 33). A dose of  $4 \times 10^7$  PFU in a final volume of 100 µl was administered 1 week after the final immunization. Viral titers were determined using HFFF-tet cells as described previously (34).

*Immunoassays for IFN-γ.* Mouse splenocytes were isolated 1 week after the final immunization. Briefly, spleens were mashed through a cell strainer (Falcon) and spun down for 10 minutes at 800 g. Viable lymphocytes were then isolated using Lympholyte Cell Separation Medium (Cedarlane). For quantification by flow cytometry, splenocytes were stimulated with the OVA peptide SL8 (2 µM) for 6 hours at 37°C. Brefeldin A was added at a final concentration of 10 µg/ml after 2 hours to prevent the secretion of IFN-γ. Cells were then stained with 7-AAD (Thermo Fisher Scientific) and α-CD8-PacBlue (clone 53-6.7, BioLegend), fixed with 4% paraformaldehyde for 20 minutes at 4°C, permeabilized with 0.1% saponin buffer for 10 minutes at 4°C, and stained intracellularly with α-IFN-γ-Alexa Fluor 700 (clone XMG1.2, BioLegend). For quantification by ELISpot assay, precoated mouse IFN-γ ELISpot<sup>PLUS</sup> plates (Mabtech) were blocked with medium containing 10% FBS for 3 hours at room temperature and then washed 4 times with PBS. Splenocytes were resuspended at  $3 \times 10^5$  cells in 100 µl R10/well and stimulated with the HIV-1 Gag p24 peptide AI9 (15 µM). After incubation for 20 hours at 37°C, the plates were washed 4 times with PBS and developed according to the manufacturer's instructions (Mabtech). Spot-forming units were counted using a BioReader 5000 (Bio-Sys GmbH).

*Statistics.* Univariate statistical analyses were performed using Prism software (GraphPad). Groups were compared using parametric tests if the data were distributed normally or nonparametric tests if the data were not distributed normally.  $P$  values less than 0.05 were considered significant.

*Study approval.* Human studies were approved by the Comité de Protection des Personnes of the Pitié Salpêtrière Hospital (France) and the Ethical Committee of Kumamoto University (Japan). Written informed consent was obtained from all donors according to the Declaration of Helsinki. Animal studies were approved by the Comité d'Ethique en Expérimentation Animale de la Loire (France) and the Ethics Committee of the National Institutes of Biomedical Innovation, Health and Nutrition (Japan).

## Author contributions

AG designed and performed experiments, analyzed data, and wrote the manuscript. LP designed and performed experiments, analyzed data, and wrote the manuscript. FN designed and performed experiments and analyzed data. TK performed experiments and analyzed data. NK designed and performed experiments and analyzed data. MPCP designed and performed experiments and analyzed data. NR designed experiments. EG performed experiments. TL performed experiments. DAP designed experiments and wrote the manuscript. EP designed experiments. MT designed experiments and analyzed data. BV designed experiments. TY designed and performed experiments and analyzed data. SP designed experiments, analyzed data, and wrote the manuscript. VA designed experiments, analyzed data, and wrote the manuscript.

## Acknowledgments

This work was supported by the French Agence Nationale de la Recherche (ANR-14-CE14-0030-01), the French Agence Nationale de la Recherche sur le SIDA (ANRS), Sidaction, Grants-in-Aid for Scientific Research and an AIDS International Collaborative Research Grant from the Ministry of Education,

Culture, Sports, Science and Technology (Japan), and a Grant-in-Aid for Young Scientists from the Japan Society for the Promotion of Science (JP17H05087). DAP is a Wellcome Trust Senior Investigator (100326/Z/12/Z). The following reagent was obtained through the NIH AIDS Reagent Program, Division of AIDS, National Institute of Allergy and Infectious Diseases: vDK1 from Daniel R. Kuritzkes.

Address correspondence to: Victor Appay. CIMI-INSERM, 91 Bd de l'hôpital, 75013, Paris, France. Phone: 33.140778183. Email: victor.appay@inserm.fr.

1. Appay V, Douek DC, Price DA. CD8+ T cell efficacy in vaccination and disease. *Nat Med*. 2008;14(6):623–628.
2. Gutjahr A, Tiraby G, Perouzel E, Verrier B, Paul S. Triggering intracellular receptors for vaccine adjuvantation. *Trends Immunol*. 2016;37(9):573–587.
3. Knudsen NP, et al. Different human vaccine adjuvants promote distinct antigen-independent immunological signatures tailored to different pathogens. *Sci Rep*. 2016;6:19570.
4. Corrales L, McWhirter SM, Dubensky TW Jr, Gajewski TF. The host STING pathway at the interface of cancer and immunity. *J Clin Invest*. 2016;126(7):2404–2411.
5. Hanson MC, et al. Nanoparticulate STING agonists are potent lymph node-targeted vaccine adjuvants. *J Clin Invest*. 2015;125(6):2532–2546.
6. Wang Z, Celis E. STING activator c-di-GMP enhances the anti-tumor effects of peptide vaccines in melanoma-bearing mice. *Cancer Immunol Immunother*. 2015;64(8):1057–1066.
7. Carroll EC, et al. The vaccine adjuvant chitosan promotes cellular immunity via DNA sensor cGAS-STING-dependent induction of type I interferons. *Immunity*. 2016;44(3):597–608.
8. Landi A, et al. Superior immunogenicity of HCV envelope glycoproteins when adjuvanted with cyclic-di-AMP, a STING activator or archaeosomes. *Vaccine*. 2017;35(50):6949–6956.
9. Cerboni S, et al. Intrinsic antiproliferative activity of the innate sensor STING in T lymphocytes. *J Exp Med*. 2017;214(6):1769–1785.
10. Li XD, Wu J, Gao D, Wang H, Sun L, Chen ZJ. Pivotal roles of cGAS-cGAMP signaling in antiviral defense and immune adjuvant effects. *Science*. 2013;341(6152):1390–1394.
11. Lissina A, et al. Priming of qualitatively superior human effector CD8+ T cells using TLR8 ligand combined with FLT3 ligand. *J Immunol*. 2016;196(1):256–263.
12. Pittet MJ, et al. High frequencies of naive Melan-A/MART-1-specific CD8(+) T cells in a large proportion of human histocompatibility leukocyte antigen (HLA)-A2 individuals. *J Exp Med*. 1999;190(5):705–715.
13. Rosalia RA, et al. Dendritic cells process synthetic long peptides better than whole protein, improving antigen presentation and T-cell activation. *Eur J Immunol*. 2013;43(10):2554–2565.
14. Glimcher LH, Townsend MJ, Sullivan BM, Lord GM. Recent developments in the transcriptional regulation of cytolytic effector cells. *Nat Rev Immunol*. 2004;4(11):900–911.
15. Coffman RL, Sher A, Seder RA. Vaccine adjuvants: putting innate immunity to work. *Immunity*. 2010;33(4):492–503.
16. Crouse J, Kalinke U, Oxenius A. Regulation of antiviral T cell responses by type I interferons. *Nat Rev Immunol*. 2015;15(4):231–242.
17. Martin TL, Jee J, Kim E, Steiner HE, Cormet-Boyaka E, Boyaka PN. Sublingual targeting of STING with 3'3'-cGAMP promotes systemic and mucosal immunity against anthrax toxins. *Vaccine*. 2017;35(18):2511–2519.
18. Takaki H, et al. cGAMP promotes germinal center formation and production of IgA in nasal-associated lymphoid tissue. *Med Sci (Basel)*. 2017;5(4):35.
19. Kinkead HL, et al. Combining STING-based neoantigen-targeted vaccine with checkpoint modulators enhances antitumor immunity in murine pancreatic cancer. *JCI Insight*. 2018;3(20):e122857.
20. Lirussi D, et al. Type I IFN and not TNF, is essential for cyclic di-nucleotide-elicited CTL by a cytosolic cross-presentation pathway. *EBioMedicine*. 2017;22:100–111.
21. Liu H, et al. Structure-based programming of lymph-node targeting in molecular vaccines. *Nature*. 2014;507(7493):519–522.
22. Lynn GM, et al. In vivo characterization of the physicochemical properties of polymer-linked TLR agonists that enhance vaccine immunogenicity. *Nat Biotechnol*. 2015;33(11):1201–1210.
23. Pavot V, et al. Recent progress in HIV vaccines inducing mucosal immune responses. *AIDS*. 2014;28(12):1701–1718.
24. Altman JD, et al. Phenotypic analysis of antigen-specific T lymphocytes. *Science*. 1996;274(5284):94–96.
25. Price DA, et al. Avidity for antigen shapes clonal dominance in CD8+ T cell populations specific for persistent DNA viruses. *J Exp Med*. 2005;202(10):1349–1361.
26. Martinuzzi E, et al. acDCs enhance human antigen-specific T-cell responses. *Blood*. 2011;118(8):2128–2137.
27. Whelan JA, et al. Specificity of CTL interactions with peptide-MHC class I tetrameric complexes is temperature dependent. *J Immunol*. 1999;163(8):4342–4348.
28. Papagno L, Almeida JR, Nemes E, Autran B, Appay V. Cell permeabilization for the assessment of T lymphocyte polyfunctional capacity. *J Immunol Methods*. 2007;328(1-2):182–188.
29. Pavot V, et al. Directing vaccine immune responses to mucosa by nanosized particulate carriers encapsulating NOD ligands. *Biomaterials*. 2016;75:327–339.
30. Pavot V, et al. Encapsulation of Nod1 and Nod2 receptor ligands into poly(lactic acid) nanoparticles potentiates their immune properties. *J Control Release*. 2013;167(1):60–67.
31. Rochereau N, et al. Delivery of antigen to nasal-associated lymphoid tissue microfold cells through secretory IgA targeting local dendritic cells confers protective immunity. *J Allergy Clin Immunol*. 2016;137(1):214–222.e2.

32. Chakrabarti S, Brechling K, Moss B. Vaccinia virus expression vector: coexpression of beta-galactosidase provides visual screening of recombinant virus plaques. *Mol Cell Biol.* 1985;5(12):3403–3409.
33. McFarland EJ, Curiel TJ, Schoen DJ, Rosandich ME, Schooley RT, Kuritzkes DR. Cytotoxic T lymphocyte lines specific for human immunodeficiency virus type 1 Gag and reverse transcriptase derived from a vertically infected child. *J Infect Dis.* 1993;167(3):719–723.
34. Stanton RJ, et al. Reconstruction of the complete human cytomegalovirus genome in a BAC reveals RL13 to be a potent inhibitor of replication. *J Clin Invest.* 2010;120(9):3191–3208.